Placenta (2005), **26**, 129–137
doi:10.1016/j.placenta.2004.05.010

Ultrasonic Detection and Developmental Changes in Calcification of the Placenta During Normal Pregnancy in Mice

C. Akirav[a,b], Y. Lu[a], J. Mu[a], D. W. Qu[a], Y. Q. Zhou[c], J. Slevin[a,d], D. Holmyard[a], F. S. Foster[c,e,f] and S. L. Adamson[a,b,d,*]

[a] Samuel Lunenfeld Research Institute of Mount Sinai Hospital, Toronto, Ontario, Canada; [b] Department of Physiology, The University of Toronto, Toronto, Ontario, Canada; [c] Mouse Imaging Centre of the Hospital for Sick Children, Toronto, Ontario, Canada; [d] Department of Obstetrics and Gynecology, The University of Toronto, Ontario, Canada; [e] Sunnybrook and Women's College Health Sciences Centre, Toronto, Ontario, Canada; [f] Department of Medical Biophysics, The University of Toronto, Toronto, Ontario, Canada

Paper accepted 19 May 2004

High resolution ultrasound imaging of the mouse placenta during development revealed highly echogenic foci localized near the materno-placental interface in early gestation and, near term, in the placental labyrinth (the exchange region of the placenta). Echogenic foci and calcium deposits identified in histological sections using Alizarin red staining showed similar localization and changes with gestation. Calcium deposits caused the echogenic foci because incubating uteri in a decalcifying solution eliminated both the deposits and echogenic foci. Transmission electron microscopy, X-ray microanalysis, and electron diffraction were used to show that deposits were calcium hydroxyapatite crystals. Calcium deposits were extensive and densely packed at days 7.5–9.5 of gestation at the border between the maternal decidua and the fetal trophoblast giant cells of ectoplacental cone. After the formation of the chorio-allantoic placenta (~day 10.5), calcification deposits appeared larger and more rarefied but were still localized at the border between the maternal decidua and the fetal trophoblast giant cells of the placenta. Calcification deposits were not observed in the labyrinthine region of the mouse placenta until ≥day 15.5 (day 18.5 is full term). We conclude that deposits of calcium hydroxyapatite crystals in the mouse placenta are detectable by high resolution ultrasound imaging. These deposits provide an ultrasound detectable marker of the maternal–placental interface that is particularly prominent during the establishment of the chorio-allantoic placenta between days 7.5 and 9.5 of gestation.
Placenta (2005), **26**, 129–137

INTRODUCTION

Successful placentation is a prerequisite for the normal progression of pregnancy, and for normal embryonic and fetal development. Indeed, in human pregnancy abnormal placentation is believed to underlie important clinical problems including early pregnancy loss, preeclampsia and intrauterine growth restriction. An important step in advancing our understanding of the etiology of these disorders is to determine the genetic regulation of normal placental development as well as the effects that abnormal regulation have on placental structure and function. Strong parallels in placental development and structure between mice and humans [1,2] suggest that genetically modified mouse models will be useful for pursuing this task. Already more than 50 mutant mouse models exhibiting abnormal placentation have been discovered [1,2]. Some are embryonic lethal (e.g. cause early pregnancy loss) [2], whereas others result in maternal symptoms similar to preeclampsia [3], and/or result in reduced fetal growth (e.g. Ref. [4]).

Exploiting these models as tools for understanding the etiology of abnormal placentation in humans necessitates investigation of placental structure and function in mice. Non-invasive, in vivo methods are especially valuable because they allow longitudinal studies of development, disease progression, and/or effects of treatments or other interventions. The ultrasound biomicroscope (UBM) uses high frequency ultrasound to non-invasively generate high resolution images of the ectoplacental cone and chorio-allantoic placenta in vivo in pregnant mice [5]. This technique has also been used to monitor blood velocity in the umbilical vessels of the embryo by Doppler ultrasound as early as the day when umbilical blood flow begins [6].

We imaged the mouse placenta throughout development using the UBM and noticed highly echogenic foci localized

* Corresponding author. Samuel Lunenfeld Research Institute of Mount Sinai Hospital, Room 138-P, 600 University Avenue, Toronto, Ontario, Canada M5G 1X5. Tel.: +1-416-586-8377; fax: +1-416-586-5993.
E-mail address: adamson@mshri.on.ca (S.L. Adamson).

0143–4004/$–see front matter

near the materno-placental interface in early gestation, and in the placental labyrinth (the exchange region of the placenta) closer to term. In the current study, we describe the echogenicity of these foci as a function of ultrasound frequency and gestational age, and show that they result from placental calcification deposits.

MATERIALS AND METHODS

The experimental procedures were approved by the Animal Care Committee of Mount Sinai Hospital and were conducted in accord with the guidelines of the Canadian Council of Animal Care (CCAC). Female ICR mice (outbred strain; Harlan Sprague Dawley, Indianapolis, IN) were bred overnight and the presence of a vaginal plug on the morning following mating was considered day 0.5 of gestation. Mice of this strain usually deliver at the end of day 18.5 of gestation.

Ultrasound imaging

Pregnant mice were anesthetized with ~1.5% isoflurane (Abbott Laboratories, Ltd., Montreal, Canada) in oxygen during ultrasound imaging. Maternal rectal temperature was monitored and maintained at 37 ± 1 °C on a heated platform supplemented with a heat lamp. The lower abdomen was shaved and any remaining hair removed using a chemical hair removal cream (Nair; Carter-Horner Inc., Mississauga, Canada). The ultrasound biomicroscope (UBM) (Model VS40 or Vevo660, VisualSonics, Toronto, Canada; www.visualsonics.com) was used to obtain two-dimensional images as previously described [5]. The height of the transducer was adjusted to place the region containing the echogenic foci within the focal zone of the transducer (where the image is brightest and the resolution the highest). In most studies, transcutaneous imaging was performed using ultrasound gel as a coupling medium. In a few studies, the uterus was exposed in a saline bath so that higher frequencies could be used to obtain higher resolution images.

Ultrasound imaging of echogenic foci as a function of gestational age

Isoflurane-anesthetized pregnant mice were imaged either transcutaneously or following exposure of the uterus between 6.5 and 18.5 days of gestation to qualitatively evaluate the distribution of the echogenic foci as a function of gestational age and ultrasound frequency.

Quantification of echogenicity

For this study, isoflurane-anesthetized pregnant mice were imaged transcutaneously every 2 days from 9.5 to 17.5 days of gestation ($n = 4$ at each age). 'Echogenicity', defined in this study as the image brightness with all gain settings held constant during acquisition and analysis, was determined as a function of transducer driving frequency and gestational age. We quantified the echogenicity of the foci near the maternal–placental interface and the average echogenicity over the entire focal zone region (to provide a measure of 'background' echogenicity). Eight similar images of the region of interest were saved for two embryos per mouse at each transducer driving frequency on the UBM (19, 25, 40 and 55 MHz). Echogenicity (image brightness) was analyzed using PhotoShop (Version 5.5, Adobe Systems Inc., San Jose, California, USA; www.adobe.com). The echogenicity of individual foci was determined after circumscribing each one using the "highlight" function key on a zoomed-in region of the image. The average echogenicity of the focal zone region was determined by using the "highlight" function key to define a 1 mm wide band centered 4 mm from the top of each image (thereby capturing the entire focal zone region). The mean gray-scale value for pixels within the highlighted area was recorded. Gray-scale values from eight similar images were averaged to give a single value of echogenicity for the area of interest at one frequency and one gestational age. A two-way analysis of variance (ANOVA) using frequency and gestational age as factors was followed by a Student–Newman–Keuls multiple comparison test (SigmaStat; SPSS, Chicago, Illinois, USA). $P < 0.05$ was considered statistically significant. Results show the mean ± SEM where n is the number of embryos.

Tissue decalcification study

Pregnant ICR mice at 7.5 ($n = 2$) and 18.5 ($n = 2$) days of gestation were euthanized by cervical dislocation. The whole bicornate uterus was removed, then horns were pinned on a layer of solidified 4% agarose, one in each of two petri dishes. Phosphate buffered saline (PBS) was added to serve as a coupling medium. Three implantation sites in each uterine horn were imaged with the UBM at 55 MHz (session 1). The uteri were fixed in 70% ethanol overnight at 4 °C then imaged in PBS the next day (session 2). After imaging the implantation sites, one horn from each mouse was placed in a 50:50 mixture of 10% formic acid (a decalcifying solution) and 70% ethanol and the other was placed in a 50:50 mixture of PBS and 70% ethanol (as a control). Uteri remained in these solutions overnight at 4 °C. On the following 3 days, the solutions were removed and the uteri were imaged in PBS. Solutions of PBS/ethanol or decalcifying solution/ethanol as appropriate were refreshed daily after each imaging session. After imaging on the final day (session 5), uterine horns were fixed in 10% buffered formalin and processed for light microscopy as described below.

Light microscopy

Implantation sites from additional mice killed at gestational ages ranging from 6.5 to 18.5 days of gestation (one to three mice at each age) were fixed in 10% buffered formalin, dehydrated in ethanol, paraffin-embedded, then serially sectioned and stained with hematoxylin and eosin (H&E), Alizarin red S or von Kossa. The von Kossa stains ferric salts as well as calcium whereas Alizarin red only stains calcium (at pH ~4.3 as in the current

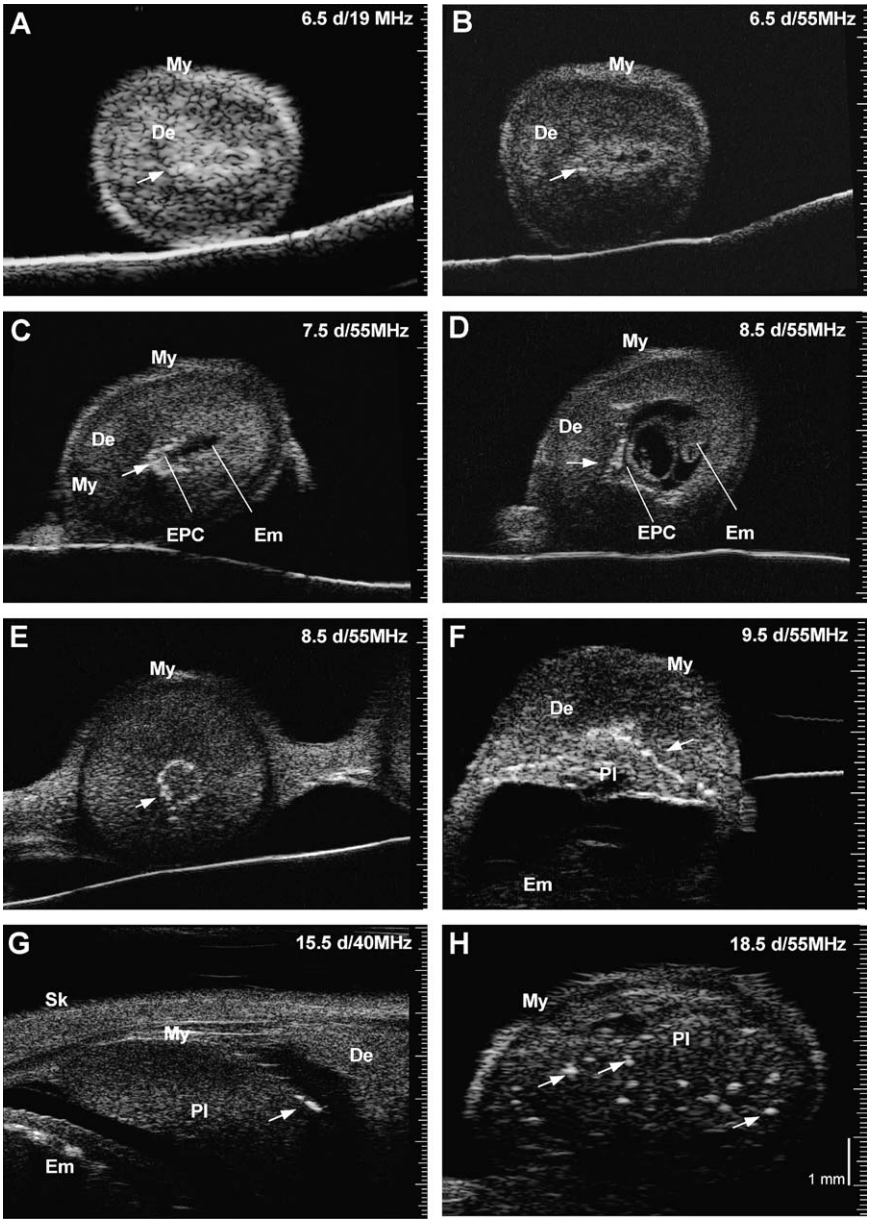

Figure 1. Ultrasound images of implantation sites viewed in vivo in exteriorized uteri at 19 MHz (A) and 55 MHz (B) at 6.5 days of gestation. Note that the image in (A) at 19 MHz is brighter but has lower resolution than image in (B) at 55 MHz. Remaining ultrasound images were obtained in vivo in exteriorized uteri at 55 MHz (B–F, H) with the exception of (G) which was obtained transcutaneously at day 15.5 at 40 MHz. Echogenic foci were prominent near the maternal–fetal interface from 7.5 to 9.5 days of gestation (C–F). Individual foci were brighter but sparser in this region in older placentas (e.g. 15.5 d (G)). Numerous echogenic foci were observed throughout the labyrinth at term (e.g. 18.5 d (H)) whereas foci were largely absent in this region earlier in gestation (e.g. 15.5 d (G)). De, decidua; Em, embryo; EPC, ectoplacental cone; My, myometrium; Pl, placenta; Sk, skin. Arrows point to echogenic foci. Smallest division on scale bars is 100 μm.

study). Sections of implantation sites were stained with Alizarin red and the location and relative amount of calcification were assessed as a function of gestational age.

Electron microscopy

One pregnant ICR mouse was euthanized at day 8.5 of gestation and the uterus was removed, fixed in 2% glutaraldehyde, dehydrated and paraffin-embedded. One implantation site was sectioned until the ectoplacental cone region was at the surface of the paraffin block. The region where calcification deposits were normally most prominent was removed from the face of the wax block, dewaxed and then embedded in plastic. Semi-thin sections were stained with toluidine blue to show tissue morphology and the presence of minerals. Thin sections were viewed using a transmission electron microscope (Model CM100; FEI) to image the mineral deposits. Composition of the deposits was analyzed by energy-dispersive X-ray spectroscopy and the crystal matrix was studied by selected area electron diffraction (Model Tecnai 20; FEI).

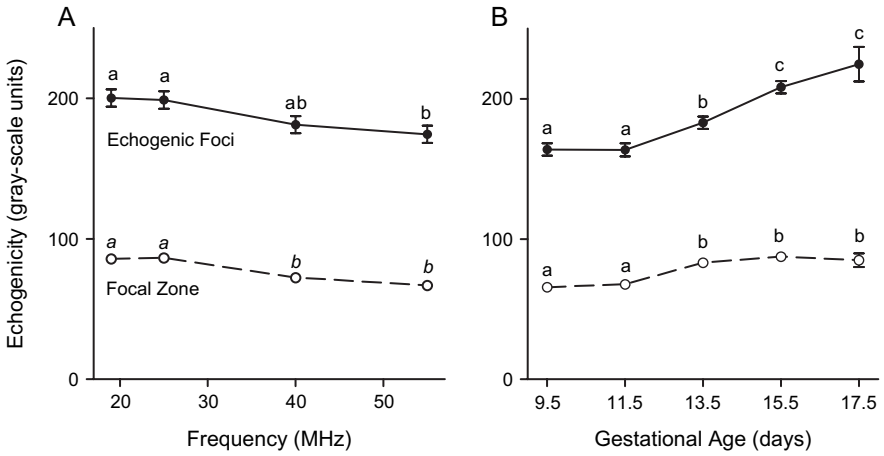

Figure 2. Echogenicity of echogenic foci near the materno-placental interface (solid line) and the focal zone region (dashed line) of ultrasound images as a function of (A) transducer driving frequency and (B) gestational age. For each variable, points that do not share the same letter significantly differ ($P < 0.05$ by two-way ANOVA). There was no significant interaction between frequency and age in echogenicity so results for all ages are pooled in (A) and results for all frequencies are pooled in (B).

RESULTS

Ultrasound imaging of echogenic foci as a function of gestational age

At day 6.5 of gestation, a slightly brighter echogenic ring was observed around implantation sites in the uterus near the trophoblast–decidual interface. The uterine image was brighter at lower transducer driving frequencies but had better resolution when viewed at higher frequencies (e.g. 19 vs 55 MHz in Figure 1A and B). At this stage, the circumference of the ring was fairly uniform in brightness although the mesometrial side (i.e. the side where the placenta will develop) was usually brighter than the antimesometrial side. By day 7.5, bright echogenic foci were primarily localized near the mesometrial side of the implantation site (Figure 1C). On day 8.5, the foci were localized in a dense cone-shaped region (V-shaped in longitudinal section, ring-shaped in cross-section) that appeared to border the ectoplacental cone (a region

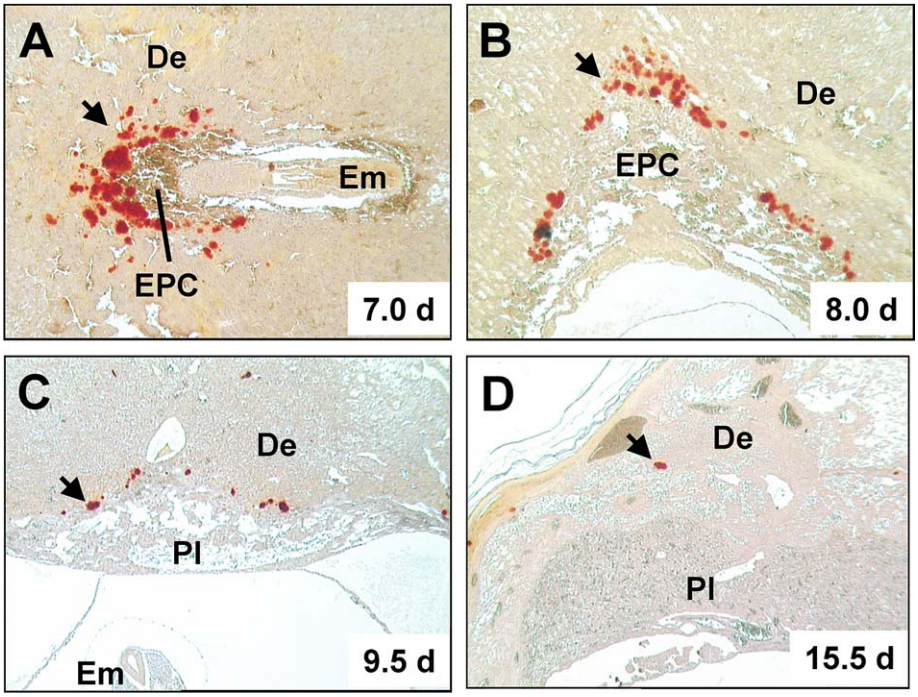

Figure 3. Light micrographs of sections through implantation sites obtained at the gestational ages indicated in each panel. Calcification deposits (stained red in images) were concentrated near the edge of the ectoplacental cone at days 7.0 and 8.0 (A, B). Later in gestation, deposits were more disperse and localized near the materno-placental interface as shown here at days 9.5 and 15.5 (C, D). De, decidua; Em, embryo; EPC, ectoplacental cone; Pl, placenta. Arrows point to calcification deposits.

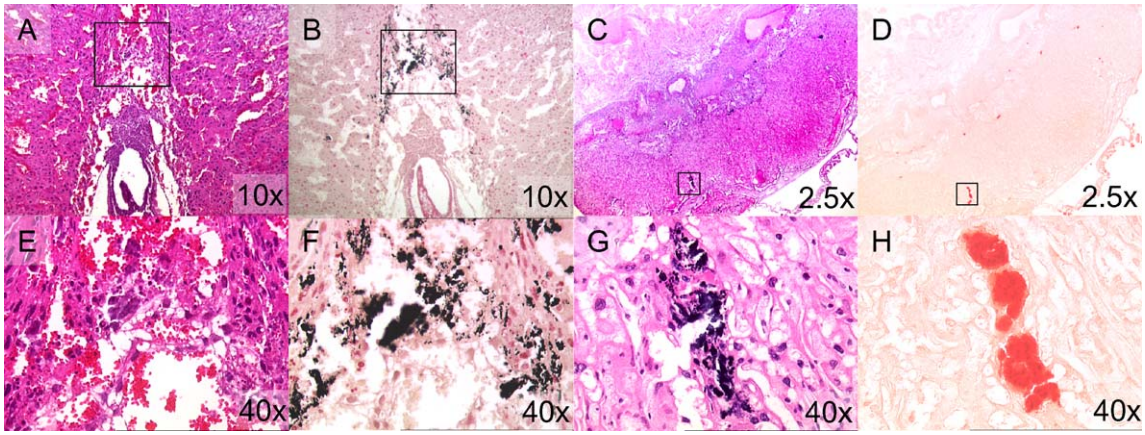

Figure 4. Light micrographs of sections through implantation sites at 7.5 days of gestation viewed at low power (A, B) and high power (E, F), and through the placenta at 18.5 days of gestation at low power (C, D) and high power (G, H). The boxed region in (A–D) is shown below at higher power in (E–H). At day 7.5, calcification deposits in the ectoplacental cone region are visible but difficult to discern in H&E sections (A, E), but the calcification deposits were obvious in serial sections stained with von Kossa (black stain) (B, F) or Alizarin red (not shown). At day 18.5, calcification deposits in the labyrinth are readily apparent in sections stained with H&E (dark stained region) (D, G), Alizarin red (red stained region) (D, H), and von Kossa (not shown).

populated by embryonic trophoblast cells) (Figure 1D and E). Upon formation of the chorio-allantoic placenta ($\geq$9.5 days), echogenic foci appeared to reside near the materno-placental interface in ultrasound images. As gestation advanced, the echogenic foci at this location became more discrete and widely spaced, and were often visibly larger and/or 'brighter' than in images from earlier gestation (Figure 1F and G). By day 15.5, echogenic foci were sometimes visible scattered throughout the labyrinth region of the placenta. Foci were always observed in this area on the last day of gestation (day 18.5) (Figure 1H).

Quantification of echogenicity

Quantification of image brightness using Photoshop showed that the echogenic foci at the materno-placental interface were more than twice as echogenic as the average echogenicity of the focal zone region at all transducer driving frequencies (Figure 2A). Transducer driving frequency only modestly affected echogenicity over the frequency range of the instrument. The effect of frequency on echogenicity did not significantly differ between the echogenic foci and the focal zone region nor did it depend on gestational age (e.g. no significant interactions by two-way ANOVA). The ~15–20% reduction in echogenicity at higher transducer driving frequencies was likely caused by the increase in attenuation associated with higher frequency ultrasound.

Quantitative measurements of the echogenicity of foci confirmed our initial qualitative observation that foci at the materno-placental interface became brighter with advancing gestation. Echogenicity of the echogenic foci and focal zone region did not change significantly between days 9.5 and 11.5 of gestation and then echogenicity of both significantly increased at day 13.5. However, only the echogenic foci showed a further significant increase at day 15.5 of gestation (Figure 2B). On average, between 9.5 and 17.5 days of gestation, the echogenicity of the foci increased 37% whereas the echogenicity of the focal zone only increased 29%. This change in echogenicity with gestational age at the two sites was significantly different ($P < 0.001$ by two-way ANOVA).

Light microscopy

Staining histological sections of the uterus at implantation sites with Alizarin red or von Kossa from days 6.0 to 18.5 of gestation revealed the presence of mineral deposits. The deposits contained calcium because, although von Kossa stains phosphorus and carbonate salts of all sorts, Alizarin red at the pH used in the current study is specific for calcium. Furthermore, no staining was observed on adjacent slides that were decalcified by immersion in 10% formic acid for 30 min and then stained with Alizarin red or von Kossa.

Prominent calcium deposits were present at the maternal–placental interface by day 7.0 (Figure 3). Occasional deposits were observed in the placental labyrinth at day 15.5 whereas they were consistently observed at this location on day 18.5 (full term) (e.g. Figures 4 and 6C). At days 7 and 8 of gestation, calcification deposits were closely packed in a region between the maternal decidua and the trophoblast giant cell layer that borders the ectoplacental cone. Most of the deposits resided in the extracellular matrix and disturbed the surrounding tissue. However, in some sections fine granules were found within the remnants of decidual cells or trophoblast giant cells suggesting that calcification may have been initiated within cells. Deposits were visible in H&E stained sections but were more apparent in sections stained with von Kossa or Alizarin red (Figures 3A, 4 and 6A). After the formation of the chorio-allantoic placenta, calcification deposits appeared larger but were fewer in number per field and they remained localized to the materno-placental interface (Figure 3). Deposits were not detected in histological sections within the labyrinthine region of the placenta until day 15.5 of gestation. By day 18.5 they were consistently present in the labyrinth and were readily observed in H&E and Alizarin red stained sections (Figures 4 and 6C), as well as sections stained with von Kossa (not shown).

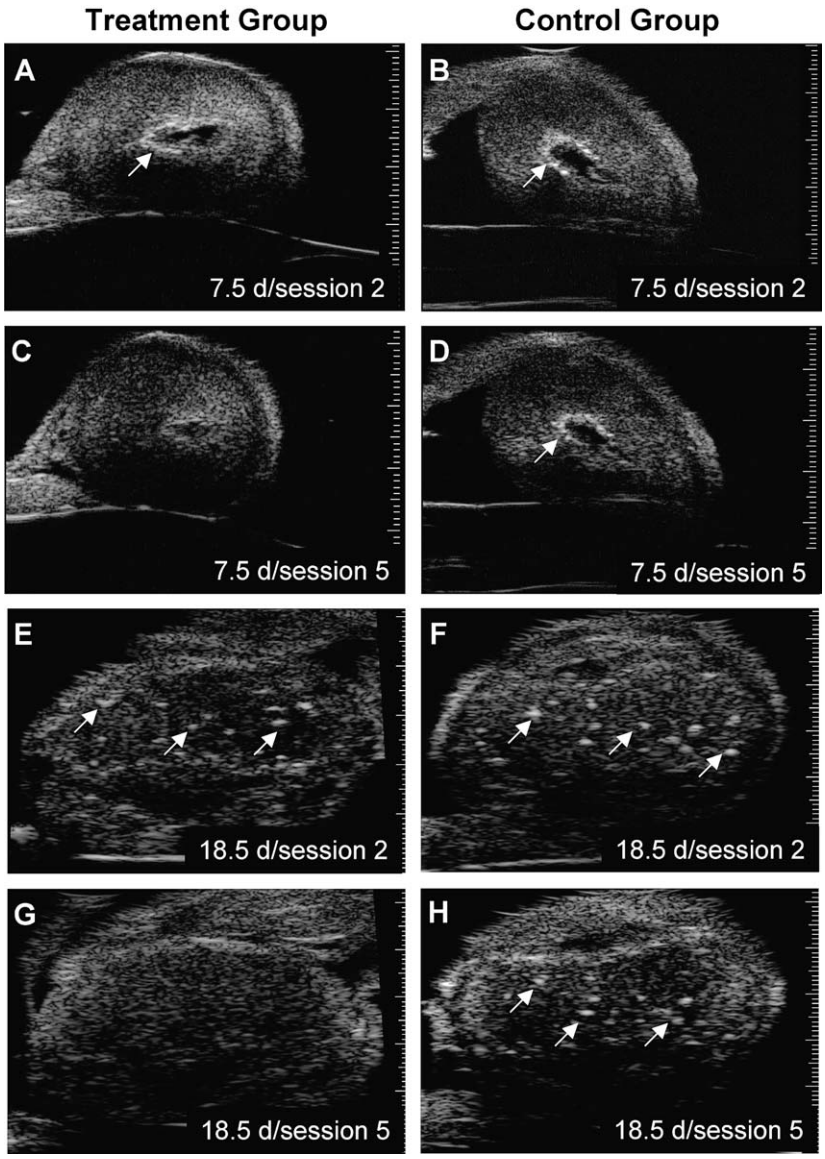

Figure 5. Ultrasound images from the implantation region of uteri at day 7.5 of gestation (A–D) or at day 18.5 (E–H) following fixation in vitro in 70% ethanol (A, B and E, F; session 2 of decalcification study). Arrows point to echogenic foci. Echogenic foci remained prominent in uterine segments from the control group (D, H) whereas treatment with a decalcification solution for 3 days resulted in a marked reduction in echogenicity in this region by session 5 of the study (C, G).

Tissue decalcification study

Changes in localization and size of echogenic foci with gestational age were strikingly similar to that of calcification deposits detected using histology. To demonstrate that the echogenic foci were calcification deposits, we imaged implantation sites ex vivo before and after treatment with a decalcification solution. We found that echogenic foci remained visible in uteri at 7.5 and 18.5 days of gestation following overnight fixation in 70% ethanol. After treating uteri for 3 days in the decalcification solution, no echogenic foci were visible whereas they were still visible in the control group at the same time-point when viewed with the UBM (Figure 5). These results suggested that the echogenic foci were generated by calcification deposits within the tissue. Furthermore, histology revealed that mineral deposits were no longer visible in Alizarin red or von Kossa stained sections from the treated uteri, whereas they were evident in control uteri (Figure 6).

Electron microscopy

Mineral deposits were visible by electron microscopy in tissue collected from the region of the ectoplacental cone at day 8.5 of gestation (Figure 7A). Spectral analysis of the mineral revealed that it contained calcium, oxygen, and phosphorous (Figure 7B) which is consistent with the mineral deposits being calcium hydroxyapatite. The electron diffraction pattern was definitive for hydroxyapatite (Figure 7C). The copper grid supporting the specimen, carbon and silicone in the support film, and carbon in the surrounding tissue caused other peaks in the spectrum (Figure 7B).

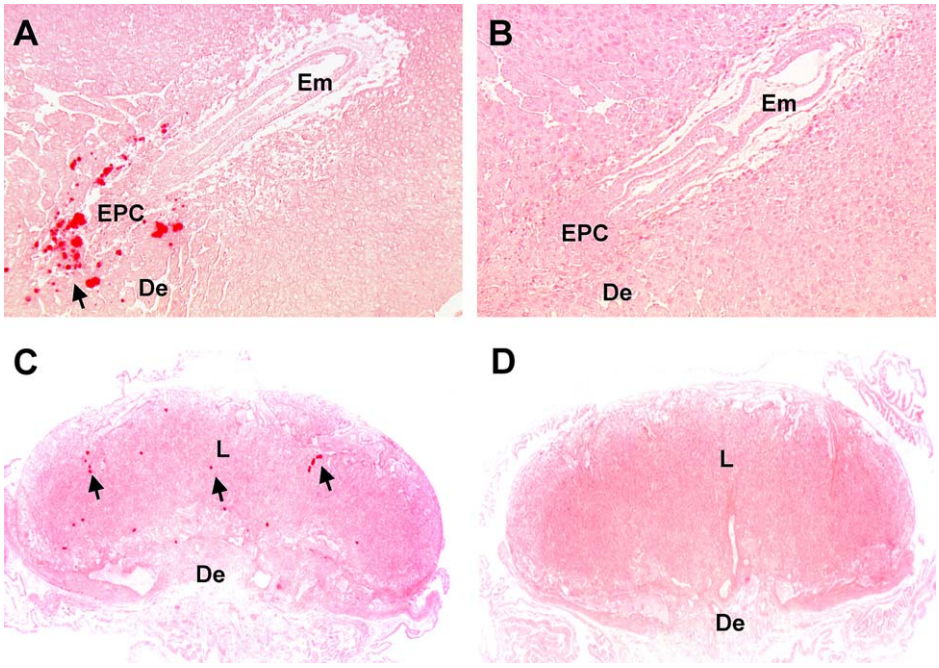

Figure 6. Representative light micrographs showing sections through the implantation region of uterine segments from day 5 of the decalcification study. Sections from the control group (A, C) and the treatment group (B, D) were stained for calcium using Alizarin red. Red staining was present near the edge of the ectoplacental cone region in the control group at day 7.5 (arrow in A) and in the labyrinth at day 18.5 (arrows in C) but staining was absent following treatment for 3 days with a decalcification solution at days 7.5 (B) and 18.5 (D) of gestation. EPC, ectoplacental cone; Em, embryo; De, decidua; L, labyrinth.

DISCUSSION

To our knowledge, this is the first report of calcification deposits in the mouse placenta. In contrast, the existence of calcification deposits in the human placenta has been known for more than 40 years [7]. Our results show that in mice, as in humans, calcification deposits are visible in ultrasound images. In humans, the echogenicity of calcification deposits constitutes an important component of Grannum grading of the placenta [9,12]. Results further show that, as in humans [8], placental calcification deposits in mice are calcium hydroxyapatite crystals.

In mice, we observed a cluster of highly echogenic calcification deposits at the implantation site prior to chorio-allantoic placental development. To our knowledge, such calcification has not been described in human pregnancy possibly because ultrasound observations at such an early stage of development are lacking. As gestation advanced in mice, calcification deposits in the region near the materno-placental interface became more rarefied. Possibly the densely packed calcification deposits bordering the ectoplacental cone laid down in early gestation were dispersed over the maternal–placental interface by the rapid growth of the chorio-allantoic placenta. Nevertheless, individual deposits along this interface became more echogenic and appeared larger on histological sections suggesting that calcium deposition slowly continued as gestation advanced.

The mechanism causing placental calcification in early gestation in the mouse is not known. However, it is possible that all three known processes of tissue calcification may be involved. In physiological calcification, as seen in bone and teeth, osteoblasts produce osteoid matrix which permits hydroxyapatite formation in and on collagen fibers. Physiologic calcification during embryonic bone formation is controlled by bone morphogenic proteins (BMPs) which also play many other important roles in development [13]. Interestingly, of the several BMPs expressed in the mouse decidua in early pregnancy, BMP7 (also known as osteogenic protein-1) is highly expressed in the mesometrial region of the decidua adjacent to the implantation site at days 7.0–7.5 of gestation [14] and thus is expressed at the same time and in the same region as the extensive calcium deposition described in the current study. BMP7 is expressed in human placental cytotrophoblast cells in early pregnancy [15] and can induce ectopic bone formation in vivo in mice [16]. Thus, BMP7, or other mediators of physiologic calcification, may induce placental calcification in this region. In dystrophic calcification, deposits form in injured or dysfunctional cells that allow extracellular calcium to enter and combine with phosphate to produce hydroxyapatite crystals. During early gestation in the mouse, implantation triggers uterine epithelial cell apoptosis and trophoblast giant cells invade and phagocytose epithelial and decidual cells [17,18]. Apoptosis and tissue damage caused by trophoblast invasion may therefore induce dystrophic calcification [19]. In metastatic calcification, deposits form in normal tissue in an environment that is supersaturated with calcium and phosphate. If active transport of calcium by placental trophoblast cells of the placenta

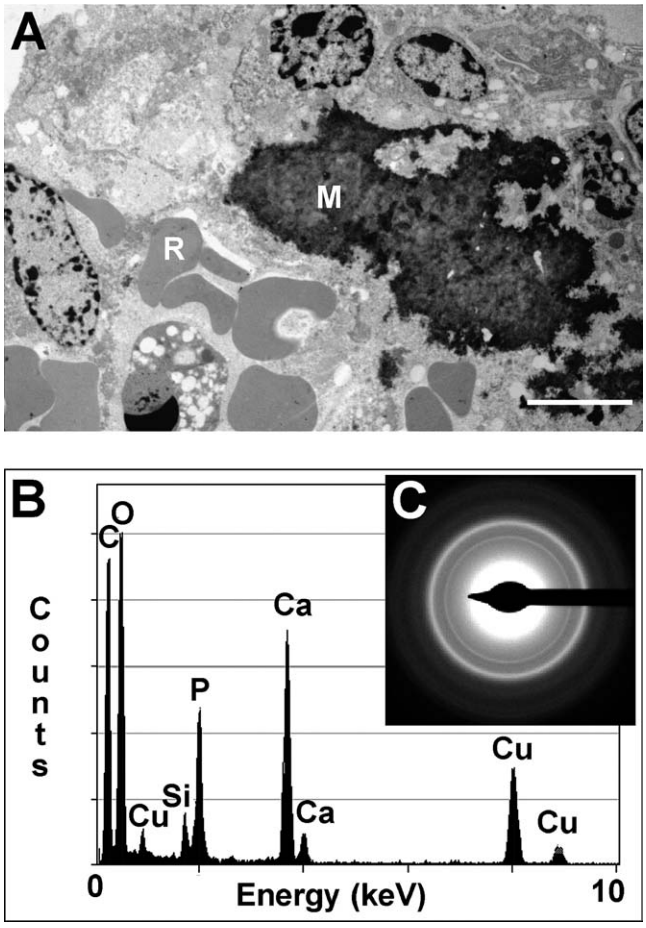

Figure 7. (A) Electron micrograph of mineral deposits located near the ectoplacental cone region of an implantation site at day 8.5 of gestation (R, red blood cell; M, mineral deposit; scale bar = 5 μm). (B) Spectrum showing the mineral composition of the deposits by energy-dispersive X-ray spectroscopy (C, carbon; O, oxygen; Cu, copper; Si, silicon; P, phosphorous; Ca, calcium). (C) Selected area electron diffraction pattern created by the crystal matrix of the mineral deposits. The mineral composition and diffraction pattern are consistent with the mineral deposits being hydroxyapatite.

[20] begins before the commencement of feto-placental perfusion (Perfusion begins on day 9.5 of gestation [6]), then high concentrations of calcium may accumulate in the vicinity of the ectoplacental cone thereby inducing metastatic calcification at this site.

In late pregnancy, we observed a progressive increase in placental calcification in the labyrinth in mice. The labyrinth is the site of maternal–fetal exchange in the mouse and thus is considered the murine counterpart of human chorionic villi [1]. Placental calcification of the chorionic villi also increases with gestational age in human pregnancy [7,10,11] and is thought to be a normal part of the maturation or aging of this organ [8]. Nevertheless, calcification begins earlier in placentas of smoking mothers, and in pregnancies complicated by preeclampsia, hypertension and intrauterine growth restriction [7,11,12], so premature calcification may contribute to or be caused by placental dysfunction [7]. It is possible that the normal increase in calcification of the labyrinth in mice and chorionic villi in humans is related to the normal gestational increase in apoptosis in trophoblast and stromal tissues of the placenta [21–23] because apoptotic bodies concentrate calcium and appear to act as nucleating structures for calcium crystal formation [19,24].

In conclusion, we have shown that dense deposits of calcium hydroxyapatite crystals are found at the maternal–fetal interface prior to the establishment of the chorio-allantoic placenta, and additional deposits appear in the placental labyrinth in late gestation in the mouse. Calcium deposits were extensive and densely packed at days 7.5–9.5 of gestation at the border between the maternal decidua and the fetal trophoblast giant cells of the ectoplacental cone. After the formation of the chorio-allantoic placenta (~day 10.5), calcification deposits at this site became larger and their occurrence more rarefied. In late gestation, calcification deposits appeared within the labyrinth region of the placenta. We further showed that calcification deposits were echogenic and clearly visible using ultrasound biomicroscopy. Deposits of calcium hydroxyapatite provide an ultrasound detectable marker of the maternal–placental interface in early pregnancy. In late pregnancy, deposition in the labyrinth may provide a useful marker of placental maturation or early degenerative changes. Thus in future longitudinal studies, ultrasound may provide a useful means to non-invasively evaluate placentation in normal and mutant mice.

ACKNOWLEDGEMENTS

This work was supported by an operating grant from the Canadian Institutes of Health Research (CIHR), and by core facilities of the CIHR Group in Development and Fetal Health. The authors also thank the Richard Ivey Foundation for funding the purchase of the UBM, and the staff at the VisualSonics Company for their technical support. We thank the Heart and Stroke Richard Lewar Centre of Excellence at the University of Toronto, and the Samuel Lunenfeld Research Institute for salary support to C. Akirav. F.S. Foster acknowledges a financial interest in the VisualSonics Company. S.L. Adamson is a member of the Scientific Advisory Board but has no financial interest in the VisualSonics Company.

REFERENCES

[1] Rossant J, Cross JC. Placental development: lessons from mouse mutants. Nat Rev Genet 2001;2:538–48.

[2] Sapin V, Blanchon L, Serre A-F, Lémery D, Dastugue B, Ward SJ. Use of transgenic mice model for understanding the placentation: towards clinical applications in human obstetrical pathologies? Transgenic Res 2001;10:377–98.

[3] Kanayama N, Takahashi K, Matsuura T, Sugimura M, Kobayashi T, Moniwa N, et al. Deficiency in $p57^{Kip2}$ expression induces preeclampsia-like symptoms in mice. Mol Hum Reprod 2002; 8:1129–35.

[4] Li Y, Behringer RR. *Esx1* is an X-chromosome imprinted regulator of placental development and fetal growth. Nat Genet 1998;20: 309–11.

[5] Zhou YQ, Foster FS, Qu DW, Zhang M, Harasiewicz KA, Adamson SL. Applications for multifrequency ultrasound biomicroscopy in mice from implantation to adulthood. Physiol Genomics 2002;10:113–26.

[6] Phoon CKL, Aristizabal O, Turnbull DH. 40 MHz Doppler characterization of umbilical and dorsal aortic blood flow in the early mouse embryo. Ultrasound Med Biol 2000;26:1275–83.

[7] Frank HG, Kaufmann P. Nonvillous parts and trophoblast invasion. In: Benirschke K, Kaufmann P, editors. Pathology of the human placenta. New York, NY: Springer-Verlag; 2000. p. 171–272.

[8] Varma VA, Kim KM. Placental calcification: ultrastructural and X-ray microanalytic studies. Scanning Electron Microsc 1985;1567–72.

[9] Grannum PA, Berkowitz RL, Hobbins JC. The ultrasonic changes in the maturing placenta and their relation to fetal pulmonic maturity. Am J Obstet Gynecol 1979;133:915–22.

[10] Poggi SH, Bostrom KI, Demer LL, Skinner HC, Koos BJ. Placental calcification: a metastatic process? Placenta 2001;22:591–6.

[11] Haney AF, Trought WS. The sonolucent placenta in high-risk obstetrics. Obstet Gynecol 1980;55:38–41.

[12] Quinlan RW, Cruz AC, Buhi WC, Martin M. Changes in placental ultrasonic appearance. II. Pathologic significance of Grade III placental changes. Am J Obstet Gynecol 1982;144:471–3.

[13] Ducy P, Karsenty G. The family of bone morphogenetic proteins. Kidney Int 2000;57:2207–14.

[14] Ying Y, Zhao G-Q. Detection of multiple bone morphogenetic protein messenger ribonucleic acids and their signal transducer, *Smad1*, during mouse decidualization. Biol Reprod 2000;63:1781–6.

[15] Martinovic S, Latin V, Suchanek E, Stavljenic-Rukavina A, Sampath KI, Vukicevic S. Osteogenic protein-1 is produced by human fetal trophoblasts in vivo and regulates the synthesis of chorionic gonadotropin and progesterone by trophoblasts in vitro. Eur J Clin Chem Clin Biochem 1996;34:103–9.

[16] Franceschi RT, Wang D, Krebsbach PH, Rutherford RB. Gene therapy for bone formation: in vitro and in vivo osteogenic activity of an adenovirus expressing BMP7. J Cell Biochem 2000;78:476–86.

[17] Bevilacqua EM, Abrahamsohn PA. Trophoblast invasion during implantation of the mouse embryo. Arch Biol Med Exp (Santiago) 1989;22:107–18.

[18] Parr EL, Tung HN, Parr MB. Apoptosis as the mode of uterine epithelial cell death during embryo implantation in mice and rats. Biol Reprod 1987;36:211–25.

[19] Kim KM. Apoptosis and calcification. Scanning Microsc 1995; 9:1137–78.

[20] Lafond J, Goyer-O'Reilly I, Laramee M, Simoneau L. Hormonal regulation and implication of cell signaling in calcium transfer by placenta. Endocrine 2001;14:285–94.

[21] Mu J, Kanzaki T, Tomimatsu T, Fukuda H, Wasada K, Fujii E, et al. Expression of apoptosis in placentae from mice lacking the prostaglandin F receptor. Placenta 2002;23:215–23.

[22] Axt R, Meyberg R, Mink D, Wasemann C, Reitnauer K, Schmidt W. Immunohistochemical detection of apoptosis in the human term and post-term placenta. Clin Exp Obstet Gynecol 1999;26:56–9.

[23] Halperin R, Peller S, Rotschild M, Bukovsky I, Schneider D. Placental apoptosis in normal and abnormal pregnancies. Gynecol Obstet Invest 2000;50:84–7.

[24] Proudfoot D, Skepper JN, Hegyi L, Bennett MR, Shanahan CM, Weissberg PL. Apoptosis regulates human vascular calcification in vitro: evidence for initiation of vascular calcification by apoptotic bodies. Circ Res 2000;87:1055–62.